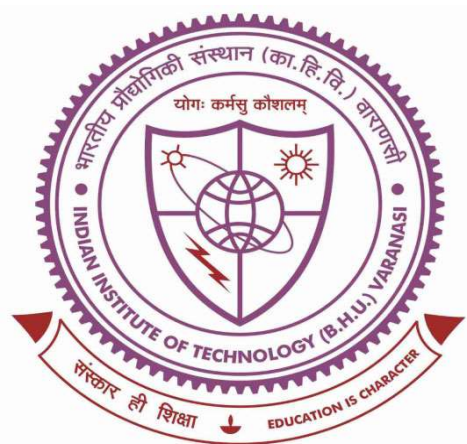


Development of novel metal-oxalate electrodes for intercalative battery type hybrid capacitor



**A thesis submitted in partial fulfillment for the
Award of Degree
Doctor of Philosophy
By**

Neeraj Kumar Mishra

**DEPARTMENT OF CERAMIC ENGINEERING
INDIAN INSTITUTE OF TECHNOLOGY
(BANARAS HINDU UNIVERSITY)
VARANASI – 221005
INDIA**

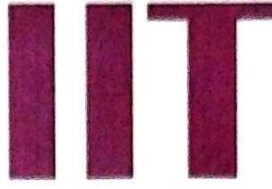
ROLL No.: 16031006

YEAR: 2022

*Dedicated to my Beloved Parents and
Family*



भारतीय
प्रौद्योगिकी
संस्थान
काशी हिन्दू विश्वविद्यालय



INDIAN
INSTITUTE OF
TECHNOLOGY
BANARAS HINDU UNIVERSITY

CERTIFICATE

It is certified that the work contained in the thesis titled *Development of novel metal-oxalate electrodes for intercalative battery type hybrid capacitor* by “*Neeraj Kumar Mishra*” has been carried out under my supervision and that this work has not been submitted elsewhere for a degree.

It is further certified that the student has fulfilled all the requirements of the comprehensive examination, candidacy, and SOTA for the award of Ph.D. Degree.


10-11-2022

Dr. Preetam Singh
Supervisor
Associate Professor,
Department of Ceramic Engineering,
Indian Institute of Technology (BHU),
Varanasi - 221005, (U.P.),

Dr. Preetam Singh
Associate Professor/सह-आचार्य
Department of Ceramic Engineering
सैरामिक अभियान्त्रिकी विभाग
Indian Institute of Technology (BHU)
भारतीय प्रौद्योगिकी संस्थान (का०हि०वि०वि०)
Varanasi-221005/वाराणसी-221005



Dr. Anil Kumar
Co-Supervisor
Associate Professor
Department of Ceramic Engineering,
Indian Institute of Technology (BHU),
India Varanasi - 221005, (U.P.), India



Head of Department
Department of Ceramic Engineering,
Indian Institute of Technology (BHU)
Varanasi - 221005, (U.P.), India
सैरामिक अभियान्त्रिकी विभाग
Indian Institute of Technology (B.H.U.)
भारतीय प्रौद्योगिकी संस्थान (का०हि०वि०वि०)
Varanasi-221005/ वाराणसी-221005



भारतीय
प्रौद्योगिकी
संस्थान
काशी हिन्दू विश्वविद्यालय



INDIAN
INSTITUTE OF
TECHNOLOGY
BANARAS HINDU UNIVERSITY

DECLARATION BY THE CANDIDATE

I, **Neeraj Kumar Mishra**, certify that the work embodied in this thesis is my own bonafide work carried out by me under the supervision of **Dr. Preetam Singh** from **July 2016** to **July 2022**, at the **Department of Ceramic Engineering**, Indian Institute of Technology (BHU), Varanasi. The matter embodied in this thesis has not been submitted for the award of any other degree/diploma.

I declare that I have faithfully acknowledged and given credits to the research workers wherever their works have been cited in my work in this thesis. I further declare that I have not willfully copied any other's work, paragraphs, text, data, results, *etc.*, reported in journals, books, magazines, reports dissertations, thesis, *etc.*, or available on websites and have not included them in this thesis and have not cited as my own work.

Signature of the student

Date: 10/11/2022

Place: IIT(BHU), Varanasi

(NEERAJ KUMAR MISHRA)

CERTIFICATE BY THE SUPERVISOR

It is certified that the above statement made by the student is correct to the best of my/our knowledge.

Dr. Preetam Singh
Supervisor
Associate Professor,
Department of Ceramic Engineering,
Indian Institute of Technology (BHU),
Varanasi - 221005, (U.P.), India

Dr. Anil Kumar
Co-Supervisor
Associate Professor
Department of Ceramic Engineering,
Indian Institute of Technology (BHU),
Varanasi - 221005, (U.P.), India

Dr. Preetam Singh
Associate Professor/सह-आचार्य
Department of Ceramic Engineering
सैरामिक अभियान्त्रिकी विभाग
Indian Institute of Technology (BHU)
भारतीय प्रौद्योगिकी संस्थान (का०हि०वि०वि०)
Varanasi-221005/वाराणसी-221005

Head of Department
Department of Ceramic Engineering,
Indian Institute of Technology (BHU)
Varanasi - 221005, (U.P.), India
सैरामिक अभियान्त्रिकी विभाग
Indian Institute of Technology (B.H.U.)
भारतीय प्रौद्योगिकी संस्थान (का०हि०वि०वि०)
Varanasi-221005/ वाराणसी-221005



भारतीय
प्रौद्योगिकी
संस्थान
काशी हिन्दू विश्वविद्यालय



INDIAN
INSTITUTE OF
TECHNOLOGY
BANARAS HINDU UNIVERSITY

COPYRIGHT TRANSFER CERTIFICATE

Title of the Thesis: *“Development of novel metal oxalate electrodes for intercalative battery type hybrid capacitor”*

Name of the Student: *Neeraj Kumar Mishra*

Copyright Transfer

The undersigned hereby assigns to the Indian Institute of Technology (Banaras Hindu University) Varanasi all rights under copyright that may exist in and for the above thesis submitted for the award of the *“DOCTOR OF PHILOSOPHY”*.

Date: 10.11.2022

Place: IIT (BHU), Varanasi

Signature of the Student

(*Neeraj Kumar Mishra*)

Note: However, the author may reproduce or authorize others to reproduce material extracted verbatim from the thesis or derivative of the thesis for the author's personal use provided that the source and the Institute's copyright notice are indicated.

Acknowledgments

The journey towards Ph.D. has been a turning point in my life, and it would not be possible without the constant support, assistance, and guidance that I have received from countless people. I would like to take this opportunity to acknowledge and appreciate those people who have given their valuable time during my Ph.D.

I am indebted to my thesis supervisor Dr. Preetam Singh for his constant monitoring, enthusiastic encouragement, continued guidance, and unconditional support throughout my Ph.D. journey. I always admire his knowledge of the subject, his unconventional thinking, and his enthusiastic nature for research. His ingenious approach to research is a source of inspiration, and this approach is reflected in his simple but clear writing style, which I want to carry forward in my career. I have been fortunate enough to be part of his group. His suggestions and advice will always be beneficial in life, whether it is academic or non-academic. I am very thankful to you sir for being a mentor academically as well as philosophically and wish to continue to seek this mentorship in future life too.

I am thankful to my RPEC members, Prof. Rajiv Prakash (SMST, IIT-BHU), Dr. Anil Kumar, and Dr. M.R. Majhi, for their knowledgeable, motivational, and umpteen suggestions throughout this research work.

I want to express my gratitude to the Ex-Head of Department, Prof. D.Kumar, and Head of Department Prof. Vinay Kumar Singh for providing me required facilities of the department. I also wish to thank all the faculty members of the Department of Ceramic Engineering, Prof. D. Kumar, Prof. Om Prakash, Prof. S.P. Singh, Prof. Ram Pyare, Prof. Vinay Kumar Singh, Dr. Anil Kumar, Dr. M. R.

Majhi, Dr. P. K. Roy, Dr. AshutoshDubey, Dr. Preetam Singh, Dr. Santanu Das, Dr. Imteyaz Ahmed, Dr. Subrta Panda, Dr. Kundan Kumar Dr. Sudama Singh, Dr. R.K. Chaturwedi, Dr.Akanksha Dwivedi, Dr. Kalyani Mohanta, for their motivation, selfless support, and suggestions during course work as well as my whole Ph.D. time.

I would also like to thank Prof. Rajiv Prakash for providing experimental facilities during the entire course of research work at CIFIC, IIT (BHU). Along with that, I am also thankful to all the staff at CIFIC, IIT(BHU).and Prof. Rajiv Prakash (SMST, IIT-BHU), Dr. T. Maiyalagan Department of Chemistry, SRM University Chennai, for their valuable discussions over the scientific work.

I would like to extend thanks to Dr. Asha Gupta, Department of Chemistry IIT(BHU) for providing a lab facility during the time of crisis. I also gratefully acknowledge the financial support of the Ministry of Education, India (formally known as the Ministry of Human Resource and Development; MHRD, India).

I am also thankful to all non-teaching staff, Mr. Shailendra, Mr. Pawan, Mr. Prasant, Mr. K. K. Maurya, (office staff)Mr. Ashish Tripathi, Mr. BhagmalJi, and Mr. Mansa Ram(all Technical and workshop staff) of the Department of Ceramic Engineering for their kind cooperation. I am very thankful to the labmates Akanksha, Rakesh, Krishna, Neeraj, Himanshu, Saurabh,and Abhay for cooperating and maintaining the lab culture. I also want to thank Dr. Asha mam research group, Vishal, Vaishali and Shraddha for their help and cooperation. I wish to express my sincere gratitude to all those who have extended their helping hands in various ways during my tenure at the Indian Institute of Technology (Banaras Hindu University),

Varanasi, India. I am also thankful for the negative energies which teach me life lessons and help me to grow.

I am highly obliged to my parent, my family, and my wife Dr. Varsha Tripathi for their continuing support, love, laughter, and motivation to keep me coherent and to make this project possible especially during many rough patches of time. I would also include my In-laws in the list for being understanding and supportive. I would like to mention my friend Mahatim, Vikas, Neeraj, Sanjo, Ashutosh, Rishi, Vipin, Sharad, Sudhanshu, Ratnesh, etc for having that emotional and motivational support during the tenure. Lastly, I want to thank almighty God for all positive opportunities and negative situations which prepare me to handle situations in the future life.

Table of Contents

List of Figures	xv
List of Tables	xxi
List of Abbreviations	xxiii
Preface.....	xxvii
Chapter 1 : Introduction	
1.1 Requirement for renewable energy	3
1.2 Renewable energy sources	3
1.2.1 Solar Energy	3
1.2.2 Wind Energy	4
1.2.3 Geothermal energy	5
1.2.4 Hydropower	6
1.2.5 Ocean energy	7
1.2.6 Bioenergy	8
1.2.7 Challenges with the renewable energy sources	8
1.3 Renewable Energy Storage Solutions	9
1.3.1 Mechanical energy storage	9
1.3.2 Hydrogen energy Storage and Methanation	10
1.3.3 Superconducting Magnetic Energy Storage (SMES)	10
1.3.4 Thermal energy storage	11
1.3.5 Electrochemical energy storage devices	12
1.3.6 Historical Perspective	12
1.3.7 Energetic of the Batteries	14
1.4 Type of rechargeable energy storage and power delivery technologies	15
1.4.1 Lead-acid battery	15
1.4.2 Lithium-ion battery	17
1.4.3 Challenges and shortcomings of Li-ion batteries	18
1.4.4 Electrochemical Supercapacitors	19
1.4.5 Electrostatic Capacitor	20

1.4.6 Supercapacitors – Electrochemical double-layer capacitors & Pseudocapacitors	21
1.4.7 Electrochemical double-layer capacitor	22
1.4.8 Principles of energy storage in EDLC	22
1.4.9 Pseudocapacitors	25
1.4.10 Principles of energy storage in pseudocapacitors	26
1.5 Electrode materials	29
1.5.1 Ruthenium dioxide (RuO₂)	30
1.5.2 Manganese dioxide (MnO₂)	31
1.5.3 Vanadium pentoxide (V₂O₅)	32
1.5.4 Nickel oxide (NiO) & nickel hydroxide (Ni(OH)₂)	33
1.5.5 Cobalt oxide (Co₃O₄) & cobalt hydroxide (Co(OH)₂)	35
1.5.6 Transition metal oxalate-based electrodes	36
1.5.7 Intercalation pseudocapacitance in Nb₂O₅	37
References	40
Chapter 2: Experimental Techniques	
2.1 Overview	53
2.2 Synthesis Technique.....	53
2.2.1 Coprecipitation synthesis route	54
2.3 Material Characterization Techniques	55
2.3.1 Powder X-ray Diffraction (XRD).....	56
2.3.2 Phase Confirmation and Crystal Structure Studies by Powder X-Ray diffraction	57
2.3.3 Scanning Electron Microscope	59
2.3.4 Transmission Electron Microscopy (TEM).....	60
2.3.5 Energy Dispersive X-Ray Spectroscopy (EDAX).....	62
2.3.6 BET (Brunner-Emmett-Teller theory) surface area measurement.....	63
2.3.7 Thermogravimetric analysis (TGA).....	64
2.3.8 Differential Scanning Calorimetry(DSC)	65

2.3.9 FTIR Spectroscopy	67
2.3.10 X-ray photoelectron spectroscopy (XPS).....	68
2.3.11 Electrochemical Measurements	69
2.3.11.1 Cyclic Voltammetry (CV)	70
2.3.11.2 Galvanostatic Charge-Discharge (GCD).....	71
2.3.11.3 Electrochemical Impedance Spectroscopy (EIS).....	72
2.3.11.4 Chemical Kinetic of pseudocapacitors from cyclic voltammetry curve..	73
References.....	76

Chapter 3 : NiC₂O₄•2H₂O Nanoflakes: A Novel Redox mediated Intercalative Pseudocapacitive Electrode for Supercapacitor Applications

3.1 Introduction.....	81
3.2 Experimental	82
3.2.1 Synthesis	82
3.2.2 Characterizations	82
3.2.3 Preparation of Electrode	83
3.3 Results and Discussions	83
3.3.1 XRD Study	83
3.3.2 SEM/EDX Study	84
3.3.3 Thermal Analysis.....	85
3.3.4 Electrochemical Studies	88
3.3.5 Two electrode test	97
3.4 Conclusions	100
References.....	102

Chapter 4 : Anhydrous CoC₂O₄ nanorods for pseudocapacitive energy storage applications

4.1 Introduction	109
4.2 Materials Synthesis and characterization.....	109
4.2.1 Synthesis	109
4.2.2 Characterizations	110

4.2.3 Preparation of Electrode	111
4.3 XRD Study	111
4.4 Thermal study	112
4.5 SEM/EDAX Study	116
4.6 Electrochemical Studies	118
4.7 Two electrode tests	127
4.8 Conclusion.....	131
References.....	132
Chapter 5: Highly Porous, Anhydrous Co_{0.5}Ni_{0.5}C₂O₄ for Pseudocapacitive Energy Storage Applications	
5.1 Introduction	139
5.2 Materials Synthesis and characterizations	140
5.2.1 Synthesis	140
5.2.2 Characterizations	140
5.2.3 Preparation of Electrode	141
5.3 XRD Study	141
5.4 Thermal study	144
5.5 SEM/EDX Study.....	148
5.6 Electrochemical Studies	150
5.7 Two electrode test	159
5.8 Conclusion	162
References.....	164
Chapter 6: Summary and Future scope	
6.1 Summary	171
6.2 Future Scope	174

LIST OF FIGURES

Figure No.	Figure description	Page No.
Figure 1.1	Solar energy working	4
Figure 1.2	wind energy	5
Figure 1.3	Geothermal energy	6
Figure 1.4	Hydrothermal energy	7
Figure 1.5	Ocean energy	7
Figure 1.6	Bioenergy	8
Figure 1.7	Structure and components of a flywheel	9
Figure 1.8	Scheme of the chemical process of hydrogen production	10
Figure 1.9	Scheme of the main component of SMES system	11
Figure 1.10	Scheme of the sensible heat storage installation	11
Figure 1.11	voltaic pile	13
Figure 1.12	Lead-acid battery	16
Figure 1.13	The configuration of a Li-ion battery is used today	17
Figure 1.14	Schematic of the simple electrostatic capacitor	20
Figure 1.15	The charge storage mechanism of EDLC	22
Figure 1.16	Double layer in (a) Helmholtz model, (b)Gouy-Chapman model, and (c) Stern model	23
Figure 1.17	Equivalent circuit diagram of Cdl in Stern model	23
Figure 1.18	Schematic of Grahame model	24
Figure 1.19	Schematic of pseudocapacitive systems identified by Conway	26
Figure 1.20	Coverage vs. the potential for positive and zero-g value	27
Figure 2.1	Flow Chart of synthesis process	55
Figure 2.2	Characterization techniques used	55
Figure 2.3	Demonstration of Bragg's Law	56
Figure 2.4	Rigaku Miniflex II, Desktop XRD Setup	57

Figure 2.5	SEM Facilities, IIT (BHU)	60
Figure 2.6	Interaction of electrons with sample	62
Figure 2.7	TEM Facilities with EDAX spectrometer, IIT (BHU)	63
Figure 2.8	BET (Brunner-Emmett-Teller theory), CIFIC. IIT(BHU)	64
Figure 2.9	TGA, IIT (BHU)	65
Figure 2.10	DSC, CIFIC. IIT(BHU)	67
Figure 2.11	FTIR Spectrometer, CIFIC. IIT(BHU)	68
Figure 2.12	X-ray photoelectron spectroscopy (XPS), CIFIC. IIT(BHU)	69
Figure 2.13	Conventional three electrodes setup used in electrochemical testing	71
Figure 2.14	Nyquist Plot for ionic solids (Z'' = imaginary impedance, Z' = real impedance)	73
Figure 2.15	Power-law dependence of the peak current on sweep rate for capacitive materials ($b= 1.0$) and typical battery-type materials ($b = 0.5$). The “transition” area between capacitive and battery-type materials area is located in the range of $b = 0.5-1.0$.	74
Figure 3.1	Powder XRD of the prepared sample of $\text{NiC}_2\text{O}_4 \cdot 2\text{H}_2\text{O}$	84
Figure 3.2	(a) FE-SEM images and (b) EDX analysis image of the prepared sample of $\text{NiC}_2\text{O}_4 \cdot 2\text{H}_2\text{O}$ sample showing flake type morphology. (c) HRTEM and (d) lattice fringes of nanoflakes type $\text{NiC}_2\text{O}_4 \cdot 2\text{H}_2\text{O}$ sample. Inset (i, ii, and iii) of (d) show FFT image, enlarged lattice fringes, and d-spacing of nanoflakes type $\text{NiC}_2\text{O}_4 \cdot 2\text{H}_2\text{O}$ sample	85
Figure 3.3	TGA of $\text{NiC}_2\text{O}_4 \cdot 2\text{H}_2\text{O}$ in N_2 atmosphere	86
Figure 3.4	FTIR of $\text{NiC}_2\text{O}_4 \cdot 2\text{H}_2\text{O}$ sample	87
Figure 3.5	BET nitrogen adsorption/desorption isotherm of $\text{NiC}_2\text{O}_4 \cdot 2\text{H}_2\text{O}$ sample.	88
Figure 3.6	(a) CV of $\text{NiC}_2\text{O}_4 \cdot 2\text{H}_2\text{O}$ electrode at 5mV/s , (b) CV curves plotted at different scan rates, (c) Plot of anodic and cathodic as a function of $v^{1/2}$, (d) Plot of rate law ($\log I$ vs $\log v$) for the two	91

	redox couples, and Trasatti plots of (e) $1/q$ vs $v^{1/2}$ and (f) q vs $v^{-1/2}$	
Figure 3.7	(a) Galvanostatic charge/discharge curve at different current densities (b) Cyclic stability graph at 5A/g for 2500 cycle and coulombic efficiency. (c) The plot of electrochemical impedance spectra (EIS) at 10mV applied potential. d) Compare CV plot in a different type of electrode nickel foam and carbon Toray paper in 2M KOH e) Compare CV study in different type electrolyte in 1M to 3M	93
Figure 3.8	(a) CV and (b) Galvanostatic charge/discharge (GCD) curve of $\text{NiC}_2\text{O}_4 \cdot 2\text{H}_2\text{O}$ electrode in 1M Na_2SO_4 electrolyte. (c) Comparative CV diagram of $\text{NiC}_2\text{O}_4 \cdot 2\text{H}_2\text{O}$ in KOH and Na_2SO_4 medium at 10mV/s, (d) Comparative charge/discharge curve of $\text{NiC}_2\text{O}_4 \cdot 2\text{H}_2\text{O}$ in KOH and Na_2SO_4 medium at 1A/g, (e) Specific capacitance of $\text{NiC}_2\text{O}_4 \cdot 2\text{H}_2\text{O}$ electrode in KOH and Na_2SO_4 electrolyte at different current density	95
Figure 3.9	(a) CV curve at different scan rates, (b) Charge-discharge curve at various current densities (c), cyclic stability and coulombic efficiency at 2A/g, and (d) plot of electrochemical impedance test at 10mV applied Potential of Activated carbon	97
Figure 3.10	(a) CV and (b) GCD, (c) cyclic stability and Coulombic efficiency of AAS cell $\text{NiC}_2\text{O}_4 \cdot 2\text{H}_2\text{O} // \text{AC}$ full cell. (d) The electrochemical impedance spectroscopy (EIS) analysis of as-prepared of $\text{NiC}_2\text{O}_4 \cdot 2\text{H}_2\text{O} // \text{AC}$ full cell before and after 1500 cycles at 10 mV of applied potential. (e) Ragone plot of $\text{NiC}_2\text{O}_4 \cdot 2\text{H}_2\text{O} // \text{AC}$ full cell showing specific energy vs. specific power.	99
Figure 4.1	(a) XRD pattern of $\text{CoC}_2\text{O}_4 \cdot 2\text{H}_2\text{O}$ and CoC_2O_4 .	112
	(b) Rietveld refinement powder XRD pattern of $\text{CoC}_2\text{O}_4 \cdot 10\text{S}$ (vista image in inset),	112
	(c) Thermogravimetric analysis (TGA) of $\text{CoC}_2\text{O}_4 \cdot 2\text{H}_2\text{O}$	113
	(d) FT-IR spectra of $\text{CoC}_2\text{O}_4 \cdot 2\text{H}_2\text{O}$ and CoC_2O_4	114
	(e) BET surface area measurement plot of $\text{CoC}_2\text{O}_4 \cdot 2\text{H}_2\text{O}$ and	115

CoC₂O₄

Figure 4.2	XPS plot of (a) full survey CoC ₂ O ₄ nanorods (b) Co (2p) (c) XPS plot of CoC ₂ O ₄ nanorods O (1s).	116
Figure 4.3	(a) SEM image showing flakes type morphology and particle size distribution of CoC ₂ O ₄ .2H ₂ O, (b) SEM image showing morphology and particle size distribution of anhydrous CoC ₂ O ₄ nanorods, (c) EDX of anhydrous CoC ₂ O ₄ nanorods, (d) TEM image at localized regions showing single rod (with FFT and inverse FFT) and (e) (110) plane d spacing of anhydrous CoC ₂ O ₄	117
Figure 4.4	(a) Cyclic voltammetry of CoC ₂ O ₄ .2H ₂ O (b) cyclic voltammetry of anhydrous CoC ₂ O ₄ nanorods (c) comparative cyclic voltammetry of CoC ₂ O ₄ .2H ₂ O and CoC ₂ O ₄ nanorods at 10 mV s ⁻¹ and (d) plot of log (peak current) vs. square root of scan rate.	120
Figure 4.5	(a) Plot of the linear relationship between log (peak current) and log(scan rate) at two different scan rate regions, (b) plot of power's law of charged state at a potential and discharged state at a potential, (c) contribution of diffusive and capacitive at different scan rates contribution, (d)analysis of kinetic contribution at 10 mV s ⁻¹ and (e and f) corresponds to Trasatti plot.	123
Figure 4.6	(a) Charge–discharge curve of CoC ₂ O ₄ .2H ₂ O, (b) charge–discharge curve of CoC ₂ O ₄ nanorods, (c) capacitance performance of CoC ₂ O ₄ nanorods at different constant current rates, (d) capacitance retention and coulombic efficiency of porous CoC ₂ O ₄ nanorods and (e) EIS plot of CoC ₂ O ₄ .2H ₂ O and porous CoC ₂ O ₄ nanorods at 10 mV	125
Figure 4.7	(a) CV and (b) charge-discharge of porous anhydrous CoC ₂ O ₄ nanorods at 10 mV s ⁻¹ in 2 M KOH and 0.5 M Na ₂ SO ₄	126
Figure 4.8	Plot for activated carbon and porous anhydrous CoC ₂ O ₄ cell in ASC mode (a) CV at 10 mV s ⁻¹ , (b) full cell CV at 10 mV s ⁻¹ with different voltage window, (c) full cell CV at different scan rate, (d) charge-discharge, (e) EIS at 10 mV, (f) capacitance retention and coulombic efficiency and (g) show plot for activated carbon and	129 130

	porous anhydrous CoC_2O_4 cell in ASC mode power density and energy density.	
Figure 5. 1	(a) XRD pattern of $\text{Co}_{0.5}\text{Ni}_{0.5}\text{C}_2\text{O}_4 \cdot 2\text{H}_2\text{O}$ and $\text{Co}_{0.5}\text{Ni}_{0.5}\text{C}_2\text{O}_4$	142
	(b) Rietveld refinement of the XRD profile of anhydrous $\text{Co}_{0.5}\text{Ni}_{0.5}\text{C}_2\text{O}_4$ (vista image in the inset)	143
	(c) Crystal structure of anhydrous $\text{Co}_{0.5}\text{Ni}_{0.5}\text{C}_2\text{O}_4$ showing tunnels for intercalation	143
	(d) TGA of $\text{Co}_{0.5}\text{Ni}_{0.5}\text{C}_2\text{O}_4 \cdot 2\text{H}_2\text{O}$ in an N_2 atmosphere (inset shows the DTA plot)	145
	(e) FT-IR spectra of $\text{Ni}_{0.5}\text{Co}_{0.5}\text{C}_2\text{O}_4 \cdot 2\text{H}_2\text{O}$ and $\text{Co}_{0.5}\text{Ni}_{0.5}\text{C}_2\text{O}_4$	146
	(f) BET surface area measurement plot of $\text{Co}_{0.5}\text{Ni}_{0.5}\text{C}_2\text{O}_4 \cdot 2\text{H}_2\text{O}$ and $\text{Co}_{0.5}\text{Ni}_{0.5}\text{C}_2\text{O}_4$	147
Figure 5.2	XPS plot of (a) full survey $\text{Co}_{0.5}\text{Ni}_{0.5}\text{C}_2\text{O}_4$, (b) Ni (2p) spectra, (c) Co 2p spectra, and (d) O (1s) spectra	148
Figure 5.3	(a) SEM image showing the morphology and particle size distribution of anhydrous $\text{Ni}_{0.5}\text{Co}_{0.5}\text{C}_2\text{O}_4$ powder; inset shows the EDX image of anhydrous $\text{Co}_{0.5}\text{Ni}_{0.5}\text{C}_2\text{O}_4$	149
	(b) TEM image at localized regions; inset shows enlarged lattice fringes (with FFT and inverse FFT) and also (110) plane d spacing of porous anhydrous $\text{Co}_{0.5}\text{Ni}_{0.5}\text{C}_2\text{O}_4$	
Figure 5.4	(a) Cyclic voltammetry of $\text{Ni}_{0.5}\text{Co}_{0.5}\text{C}_2\text{O}_4 \cdot 2\text{H}_2\text{O}$, (b) cyclic voltammetry of porous anhydrous $\text{Ni}_{0.5}\text{Co}_{0.5}\text{C}_2\text{O}_4$, (c) comparative cyclic voltammetry curves for $\text{Ni}_{0.5}\text{Co}_{0.5}\text{C}_2\text{O}_4 \cdot 2\text{H}_2\text{O}$ and $\text{Ni}_{0.5}\text{Co}_{0.5}\text{C}_2\text{O}_4$ electrodes at 10 mV/s, and (d) plot of log (peak current vs square root of the scan rate for porous anhydrous $\text{Ni}_{0.5}\text{Co}_{0.5}\text{C}_2\text{O}_4$).	151
Figure 5. 5	Electrodynamic characteristics of the $\text{Co}_{0.5}\text{Ni}_{0.5}\text{C}_2\text{O}_4$ electrode; (a) plot of the linear relationship between log (peak current) and log (scan rate) at two different scan rate regions, (b) plot of the power law of the charged state at a potential and discharged state at a potential, (c) contribution of diffusive and capacitive contribution	155

at different scan rates, (d) analysis of kinetic contribution at 10 mV/s, and (e, f) show Trasatti plot at different scan rates.

Figure 5.6 (a) Charge/discharge curve of $\text{Co}_{0.5}\text{Ni}_{0.5}\text{C}_2\text{O}_4 \cdot 2\text{H}_2\text{O}$, (b) charge/discharge curve of porous anhydrous $\text{Co}_{0.5}\text{Ni}_{0.5}\text{C}_2\text{O}_4$, (c) capacitance performance of porous anhydrous $\text{Co}_{0.5}\text{Ni}_{0.5}\text{C}_2\text{O}_4$ at different constant current rates, (d) capacitance retention and Coulombic efficiency porous anhydrous $\text{Co}_{0.5}\text{Ni}_{0.5}\text{C}_2\text{O}_4$, and (e) EIS plot and enlarged (zoom) view of the EIS plot of $\text{Co}_{0.5}\text{Ni}_{0.5}\text{C}_2\text{O}_4 \cdot 2\text{H}_2\text{O}$ and porous anhydrous $\text{Co}_{0.5}\text{Ni}_{0.5}\text{C}_2\text{O}_4$ electrode at 10 mV (AC). 158

Figure 5.7 (a) Representative CV for activated carbon (AC) and porous anhydrous $\text{Co}_{0.5}\text{Ni}_{0.5}\text{C}_2\text{O}_4$ at 10 mV/s, (b) plot for activated carbon and the porous anhydrous $\text{Co}_{0.5}\text{Ni}_{0.5}\text{C}_2\text{O}_4$ cell in ASC mode CV at different scan rates, (c) charge/discharge at different current rates, (d) EIS at 10 mV (AC), (e) capacitance retention and columbic efficiency, and (f) power density and energy density of two electrode cells in ASC mode 160

TABLES

Table No.		Page No.
Table 1.1	Development of various battery technologies	13
Table 2.1	Powder diffraction pattern as a function of various crystal structure, specimen, and instrumental parameters	59
Table 3.1	Comparison of specific energy values for different reported Aqueous Asymmetric Nickel-based positive electrode supercapacitors	100
Table 4.1:	Comparison of capacitive performances of different Cobalt oxalate based electrodes	130
Table 5.1	Comparison of capacitive performances of different oxalate based electrodes	162
Table 6.1	Showing charge storage capacity of different electrodes developed in this thesis.	174

LIST OF ABBREVIATIONS

XRD-X-ray Diffraction
HR-SEM-High-Resolution Scanning Electron Microscope
HR-TEM-High-Resolution Transmission Electron Microscope
TGA- Thermogravimetric analysis
FTIR-Fourier transform Infrared Spectroscopy
XPS-X-ray Photoelectron Spectroscopy
BET - (Brunauer, Emmett, and Teller) specific surface
CV- Cyclic Voltammetry
ASCs – Asymmetric Supercapacitors
C_{sp} - specific capacitance
A, mA (unit) - Ampere, milliamp
AC - Activated Carbon
AM - Active mass
C, μC (unit) - Coulomb, microcoulomb
C - Capacitance
C^{+/R⁺} - Cationic species in electrolyte
C* - Complex differential capacitance
C^{+ve} - Capacitance of positive electrode
C^{-ve} - Capacitance of negative electrode
C_{cell} - Overall cell capacitance
C_{Diff} - Capacitance from diffuse layer
C_{dl} - Capacitance from double layer
C_g - Gravimetric capacitance
C_H - Capacitance from Helmholtz plane
C_{IH} - Capacitance from inner Helmholtz plane
C_{OH} - Capacitance from outer Helmholtz plane
e⁻ - Electron
 ϵ - Permittivity of vacuum
E - Electrode potential

E° - Standard electrode potential

E_{Total} - Total energy stored in capacitor

EDLC - Electrochemical double layer capacitor

EIS - Electrochemical impedance spectroscopy

ES - Electrochemical supercapacitor

f - Frequency

F - Faraday constant

F, mF, μF (unit) - Farad, millifarad, microfarad

g, mg, μg (unit) - Gram, milligram, microgram

h (unit) – Hour

Hz, mHz, kHz (unit) - Hertz, millihertz, kilohertz

I - Current

K (unit) - Temperature in Kelvin

K – Boltzmann's constant

M - Mass of active materials

m, cm, μm , nm (unit) - Meter, centimeter, micrometer, nanometer

M - Molar concentration

Q - Charge stored

V - Voltage

V_{Max} - Maximum voltage

V_{Min} - Minimum voltage

W (unit) - Watt

Wh (unit) - Watt hour

wt% - Weight percentage

ω - Angular frequency

X - Fraction of ion occupancy in lattices

z - Number of electrons transferred in redox reactions

Z^* - Total impedance

Z' - Real component of impedance

Z'' - Imaginary component of impedance

ΔV - Voltage window

$^{\circ}\text{C}$ (unit) - Temperature in Celsius

θ_{H} - Surface coverage of H^+ in underpotential deposition

[Ox] - Concentration of oxidized species

[Red] - Concentration of reduced species

PREFACE

The energy supply based on fossil fuels To fulfill the ever-increasing energy demands to sustain the continuous growth and development of society has increased the inaccessible burden on fossil fuel resources and is decisively adding to climate change concerns and global warming. Renewable energy generation (including solar energy, wind energy, geothermal energy, etc.) has drawn significant attention as an alternative to fossil fuels and a remedy of concern related to pollution, global warming, and climate change due to net carbon addition to the earth environment. However, the power supply through renewable sources is irregular or fluctuating due to the time and weather-dependent nature of renewable sources and can not be used directly in electrical and electronic appliances. Though costly, yet most efficient, Electrochemical energy storage is key to harnessing the full potential of renewable energy sources, and thus grid-scale energy storage solutions are required to reduce the burden of fossil fuel-based energy solutions and instead use renewable power sources.

In this thesis, we focus on development of high energy-high power delivering redox-mediated intercalative supercapacitor to establish grid-scale energy storage solutions. In pseudocapacitors, energy is stored by fast and reversible redox reactions at the surface of active materials. Compared to EDLCs, pseudocapacitors offer 10 to 100 times higher capacitance because charge storage is not limited to the surface only, but also to the near-surface region where ions can diffuse. Pseudocapacitance arises when electrode potential is dependent logarithmically on the extent of reactions and involves charge transfer across the double layer. The intercalative pseudocapacitance is also based on redox reactions, which arise when ions intercalate into tunnels or layers of active materials accompanied by faradic charge transfer without crystallographic phase change but involve redox reactions in a 3-

dimensional structure rather than a 2-dimensional surface in redox pseudocapacitance. Metal oxalate framework structures are employed here to develop superior electrodes for hybrid intercalative battery-type supercapacitors. Thermochemical properties especially coupling of TGA/DTA techniques with strategic precipitation schemes to develop novel highly porous nanostructures that can enable fast transport or diffusion of ions in the host structure to have large-scale charge storage capabilities are employed here to develop effective electrodes for intercalative battery type supercapacitors.

$\text{NiC}_2\text{O}_4 \cdot 2\text{H}_2\text{O}$ flakes were synthesized using a single-step co-precipitation method in an aqueous medium. $\text{NiC}_2\text{O}_4 \cdot 2\text{H}_2\text{O}$ -based electrode showed intercalative charge storage behavior exhibiting specific capacitance of 990 F/g at a current density of 1 A/g with excellent cyclic stability. $\text{NiC}_2\text{O}_4 \cdot 2\text{H}_2\text{O}$ electrode showed superior specific capacitance equivalent to 990 F/g in the potential window of 0.45 V was observed in an aqueous KOH electrolyte and 440 F/g in 1M neutral Na_2SO_4 electrolyte in the potential window of 0.85 V.

Highly porous, anhydrous CoC_2O_4 nanorods were successfully synthesized using a two-step process, first $\text{CoC}_2\text{O}_4 \cdot 2\text{H}_2\text{O}$ was synthesized by co-precipitation method in an aqueous medium followed by heating the precipitate at 210 °C to produce porous CoC_2O_4 nanorods. Porous CoC_2O_4 nanorods showed pseudocapacitive energy/charge storage behavior with a specific capacitance of the materials reaching as high as 2116 F g⁻¹ at a current density of 1A g⁻¹ with excellent cyclic stability. The predominant intercalative mechanism seems to operate behind high charge storage as intercalative (inner) and surface (outer) charges stored by porous anhydrous CoC_2O_4 were close to 75% and 25% respectively. Porous anhydrous CoC_2O_4 // AC full cell resulted in maximum specific energy of 129 W h kg⁻¹ and specific power of ~647 Wkg⁻¹ at 0.5 A g⁻¹ current density in the voltage window of 1.3 V in 2 M

KOH electrolyte.

Anhydrous $\text{Co}_{0.5}\text{Ni}_{0.5}\text{C}_2\text{O}_4$ was successfully synthesized using a two-step process; first, $\text{Co}_{0.5}\text{Ni}_{0.5}\text{C}_2\text{O}_4 \cdot 2\text{H}_2\text{O}$ was synthesized by the co-precipitation method in an aqueous medium, and then $\text{Co}_{0.5}\text{Ni}_{0.5}\text{C}_2\text{O}_4 \cdot 2\text{H}_2\text{O}$ was heated at 230 °C for 5 h, which resulted in porous anhydrous $\text{Co}_{0.5}\text{Ni}_{0.5}\text{C}_2\text{O}_4$. The anhydrous $\text{Co}_{0.5}\text{Ni}_{0.5}\text{C}_2\text{O}_4$ electrode showed a highly pseudocapacitive performance with a specific capacitance of 2396 F/g at a current density of 1 A/g and excellent cyclic stability. The porous anhydrous $\text{Co}_{0.5}\text{Ni}_{0.5}\text{C}_2\text{O}_4$ //AC full cell resulted in 283 W h/kg of maximum specific energy with a specific power equivalent to 817 W/kg in the voltage window of 1.6 V in the 2 M KOH electrolyte at a 1 A/g current rate.

In this thesis, I conclude that framework structure material containing transition metal ions can be an excellent host to develop novel electrodes that can enable fast charge-discharge to develop high energy high power delivering battery type capacitors. The use of TGA/TDA techniques can be an important tool to modify the synthesis schemes to develop highly porous nanostructured materials to employ as an electrode in batteries and capacitors. Ni/Co oxalate framework was shown to have redox-mediated charge storage capability that can dissipate power or current at fast rates to power electronic and electrical appliances and to be applied as grid-scale energy storage solutions. I found that the transition metal oxalate electrodes in full cell asymmetric supercapacitor (ASC) mode where activated carbon is utilized as a negative electrode can deliver power performance and rate capabilities comparable to lead acid batteries and further studies can bring superior aqueous redox-mediated battery type capacitor that can be employed for grid-scale energy storage solution and can also be utilized as an alternate to lead acid batteries to power inverters.